

The structure of magnetic domain walls in cylindrical nano- and microwires with inhomogeneous anisotropy

Ksenia A. Chichay^{1,a}, Igor S. Lobanov^{1,b}, Valery M. Uzdin^{1,c}

¹Department of Physics, ITMO University, St. Petersburg, Russia

^aks.chichay@gmail.com, ^blobanov.igor@gmail.com, ^cv.uzdin@mail.ru

Corresponding author: K. A. Chichay, ks.chichay@gmail.com

PACS 75.60.Ch, 75.30.Gw

ABSTRACT The structure of domain walls in cylindrical nano- and microwires with a non-uniform anisotropy distribution in the transverse-radial direction has been studied. This distribution can be controlled by mechanical stresses associated with specific wire manufacturing methods as well as with the glass coating in some types of microwires. Our calculations have shown that in the presence of axial anisotropy in the core of the wire and radial anisotropy near its surface, various configurations of domain walls can be stabilized. A diagram of magnetic states has been calculated depending on the radial anisotropy values. The stability of various types of domain walls and their possible transformation under the excitation of thermal fluctuations and external perturbations are discussed.

KEYWORDS Domain wall, cylindrical systems, amorphous ferromagnetic microwires, mechanical stress, micro-magnetics.

ACKNOWLEDGEMENTS This work was funded by Russian Science Foundation (project No. 23-72-10028, <https://rscf.ru/en/project/23-72-10028/>). K.A.Ch. acknowledges the support of ITMO Fellowship Program.

FOR CITATION Chichay K.A., Lobanov I.S., Uzdin V.M. The structure of magnetic domain walls in cylindrical nano- and microwires with inhomogeneous anisotropy. *Nanosystems: Phys. Chem. Math.*, 2024, **15** (1), 55–59.

1. Introduction

Magnetic domains in nano- and microwires are of great interest in relation with the concept of racetrack magnetic memory [1–3]. In these memory devices, information is stored in the form of a sequence of domain walls (DW) that can be moved by an electric current. The absence of mechanical motion of reading and writing tools relative to the magnetic medium, the high density of domain walls, and their ability to move at high speed under the action of low currents make this technology very promising. Low-dimensional magnetic systems with cylindrical symmetry (such as nano- and microwires) are of particular interest from this point of view [4, 5]. The cylindrical shape determines a number of useful properties and advantages compared to low-dimensional planar structures. The combination of strong shape anisotropy and cylindrical symmetry makes it possible to stabilize axisymmetric states [6]. Moreover, due to the absence of edges in cylindrical wires, the DW can rotate along the axis of the wire without loss of energy, thereby preventing changes in the structure of the DW (that is, blocking nucleation of anti-vortex states, as occurs in planar wires) [4, 7]. In this way, the so-called Walker breakdown [7, 8] is suppressed, which promises higher DW speed [9, 10].

To date, three types of DWs have been discovered that can be stabilized in nano- micrometer-sized cylindrical systems with uniform magnetic parameters [6]. These are a transverse DW (which is the ground state for thin wires), a Bloch point DW (which is the ground state for thicker wires) and an asymmetric transverse DW, which can only be a metastable state.

In addition to the properties associated with cylindrical symmetry, the small spatial size of micro- and nanowires increases the role of surface and interface effects, and also allows one to significantly change the magnetic characteristics when exposed to mechanical stresses during sample manufacturing or induced anisotropy. This makes it possible to obtain media with parameters unattainable in bulk materials, which turns out to be quite useful for energy-efficient applications [11]. Examples of such cylindrical magnetic systems are amorphous ferromagnetic microwires in a glass shell, obtained by drawing from a melt [12–14]. As a consequence of the fabrication method (drawing and rapid quenching) [15], such systems, in addition to being amorphous, have internal stresses, that lead to a non-uniform distribution of anisotropy in the transverse-radial direction [16–18]. The microwires with a positive magnetostriction acquire an easy magnetization axis oriented along its axis. Such microwires are magnetically bistable (they have only two stable states corresponding to two directions of the magnetization vector along the wire), and magnetization reversal occurs by extremely fast DW movement (single Barkhausen jump) [19].

Presently, there are a lot of experimental data on the dynamics of the DW in such wires. DW velocity and mobility, critical values of external magnetic field and current required for the DW movement as well as the range of fields and

currents at which magnetization reversal occurs through the DW movement are being studied very intensively [20–22]. However, there is still no complete understanding of the types and internal structure of the DW in such systems. In experiments, only the width and approximate shape of the DW can be estimated by analyzing the emf peaks induced by the traveling DW (and, therefore, the change in magnetization) in the pick-up coils [21, 23, 24]. This is due to the “inconvenient size” of such microwires: their lateral dimensions, on the one hand, are very small, and on the other hand they are too bulky to use transmission electron microscopy or tools that can only provide information about the magnetic structure on the surface.

Presumably, in such cylindrical systems with non-uniform magnetic parameters as amorphous ferromagnetic microwires in glass shell [16] the DW structure can be more complex than that of known types of DWs in nanowires. This is due to the micrometer diameter of such wire and inhomogeneity of anisotropy along the radius, which can significantly change the configuration of DW. In this case micromagnetic simulations can play a decisive role in revealing existing magnetic configurations.

In our work, we investigated the stability and internal structure of domain walls stabilized in cylindrical wires with inhomogeneous anisotropy. We considered wires with fixed geometric parameters, but different ratios of the anisotropy values in the core and on the surface of the wire. We have shown stabilization of radial domain wall by the radial anisotropy. According to our simulations radial DW has larger stability region than the transverse DW, while their energy are close in the domain of coexistence.

2. Method

We consider a ferromagnetic wire of radius R and length L shown in Fig. 1. The total micromagnetic energy of the system in cylindrical coordinates is given by:

$$\mathcal{E} = \iiint \left(\frac{A}{2} \left[\left(\frac{\partial \mathbf{S}}{\partial \rho} \right)^2 + \frac{1}{\rho^2} \left(\frac{\partial \mathbf{S}}{\partial \phi} \right)^2 + \left(\frac{\partial \mathbf{S}}{\partial z} \right)^2 \right] - \sum_i K_i(\rho) (\mathbf{S} \cdot \mathbf{e}_i)^2 - B (\mathbf{S} \cdot \mathbf{e}_z) \right) \rho \cdot d\rho \cdot d\phi \cdot dz \quad (1)$$

where \mathbf{S} is the magnetization vector field. The first term in (1) is the exchange energy with exchange stiffness $A = 2 \cdot 10^{-11}$ J/m. The second term describes the easy-axis/easy-plane anisotropy $K_i(\rho)$, which is non-uniform along the radius ρ of the wire, and the third term is the interaction with an external magnetic field B , which is applied along the z direction. The anisotropy axis \mathbf{e}_i is assumed to be different in the core of the wire, where it coincides with the z axis \mathbf{e}_z , and near the surface, where it is assumed to be radial.

For simulations, we use the type and value of anisotropy corresponding to the anisotropy distribution in amorphous ferromagnetic microwires, but in a simplified form. Thus, according to the anisotropy distribution given in [15], starting from the center of the wire to $0.9R$, we used the average value of axial anisotropy $K_{ax} = 1 \cdot 10^4$ J/m³ (easy axis). On the periphery the radial type of anisotropy, K_r , prevails (easy axis). To investigate the influence of the anisotropy on the periphery on the type and structure of the domain wall, we vary the value of K_r from 0 to $10 \cdot 10^4$ J/m³. In addition to stress-induced anisotropy, we include an effective shape anisotropy for cylinder $K_{eff} = 1/4\mu_0 M_s^2$ due to the demagnetization field, where $M_s = 500$ kA/m is saturation magnetization.

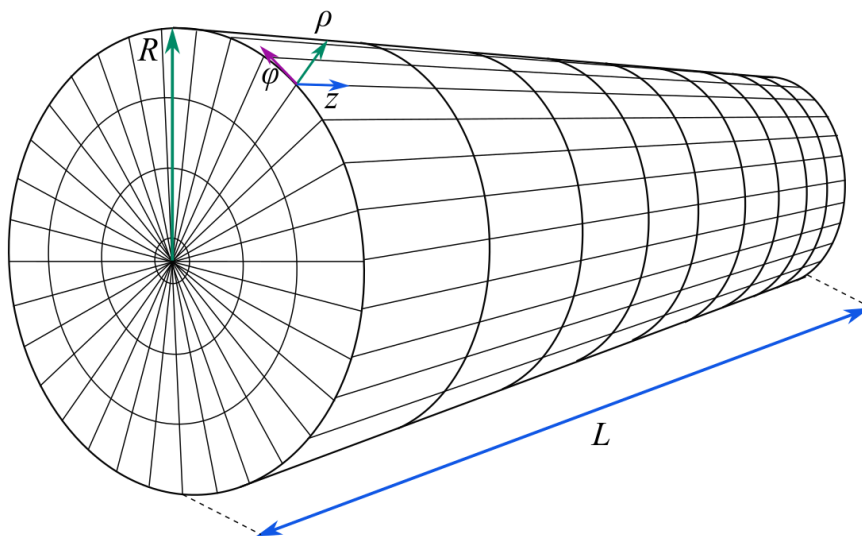


FIG. 1. Schematic representation of a wire in cylindrical coordinate system. R is the wire radius, L is the length of the wire.

The calculations were made using the original code developed by the authors, which implements a finite-difference discretization scheme. Since discretization in this way results in unit cells of different sizes, we took into account the cell volume to calculate the local magnetic moment. For simulations, we use a wire with radius $R = 0.1 \cdot 10^{-6}$ m and length $L = 1 \cdot 10^{-6}$ m with periodic boundary conditions in the z direction. The number of discretization nodes along each axes was: $N_\rho = 30$ (from the center of wire to the periphery), $N_\phi = 100$, $N_z = 400$.

3. Results

For wires with inhomogeneous anisotropy, we found two configurations of the DWs. Fig. 3 shows a 3D view and $\rho-\phi$ cross section of each of the two head-to-head DW configurations. The first configuration (Fig. 3a) is the transverse DW, similar to that found for planar and cylindrical nanowires. In this case, the transition from an axially ordered magnetization parallel to the e_z axis in one direction to ordering in the opposite direction occurs by rotating the magnetization about an axis perpendicular to the wire axis, breaking the axial symmetry. Due to the cylindrical symmetry of the wire and the absence of a preferred transverse direction, such a DW can be formed at any angle ϕ . Black and grey colors on the 3D view in Fig. 3 represent the magnetization being parallel and antiparallel to the z -axis ($+z$ and $-z$), while colors indicate the transverse component of magnetization for different ϕ angles.

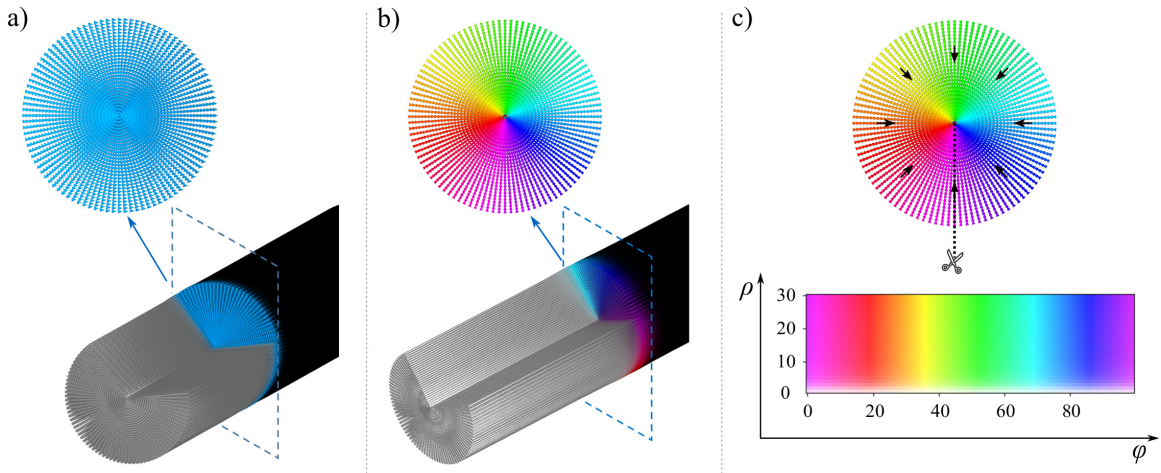


FIG. 2. 3D view and cross section of the cylindrical wire representing magnetic configuration of a) transverse DW, b) radial DW. The cross sections indicate the structure of the DWs at the marked position. Both cross sections are given for the value $K_r = 0$; c) the unrolled view of the $\rho-\phi$ cross section. Direction of magnetization is indicated by color. Black arrows in panel (c) set correspondence between direction and color.

Another type of DW corresponds to the magnetization ordered radially from or towards the center of the wire. In this case, a Bloch point is formed on the axis of symmetry, see Fig. 3b. We refer to this type of a magnetic configuration as a radial domain wall. The bottom panel of Fig. 3c shows the “unrolled” spin structures of the $\rho-\phi$ cross section for radial DW. The magnetization direction is color-encoded as indicated in upper panel in Fig. 3c.

Having discovered two DW configurations, we investigated their stability depending on the value of radial anisotropy at the near surface region of the wire. Fig. 3 summarizes our results as a phase diagram that shows the magnetic energy as a function of radial anisotropy value for both stable DW configurations. Fig. 3a represents the distribution of anisotropy types (axial and radial) along the wire radius. Almost the entire volume of the wire is dominated by the axial anisotropy, corresponding to the realistic case of amorphous ferromagnetic microwires [15]. The radial anisotropy prevails in the outermost 10% of the wire radius forming a layer with a thickness of 10 nm in the considered case.

To study the phase diagram of the obtained DW configurations depending on the anisotropy parameters, each of the DW types obtained at certain anisotropy values was taken as the initial state and relaxed to a local minimum at other anisotropy values. The phase diagram (Fig. 3b) shows that in the case of zero radial anisotropy, only the transverse DW is stable and is an ordinary transverse DW in cylindrical wires. Further, at low values of radial anisotropy, both DW configurations have very similar energy values, although the energy of the transverse DW is somewhat lower in the range of radial anisotropy values from 0 to $4.3 \cdot 10^4$ J/m. At values of K_r above $4.3 \cdot 10^4$ J/m, only the radial DW is stable, and the energy of the system decreases with increasing the radial anisotropy value.

Figure 3c shows the transverse DW for various values of radial anisotropy at the nearsurface region. A more visual representation of the magnetic structure can be obtained by unrolling the $\rho-\phi$ magnetization cross section. It can be seen that at zero radial anisotropy the DW is a conventional transverse DW, when all spins are ordered perpendicular to the wire axis with the same angle ϕ . At non-zero values of radial anisotropy, one can observe a deviation of magnetization

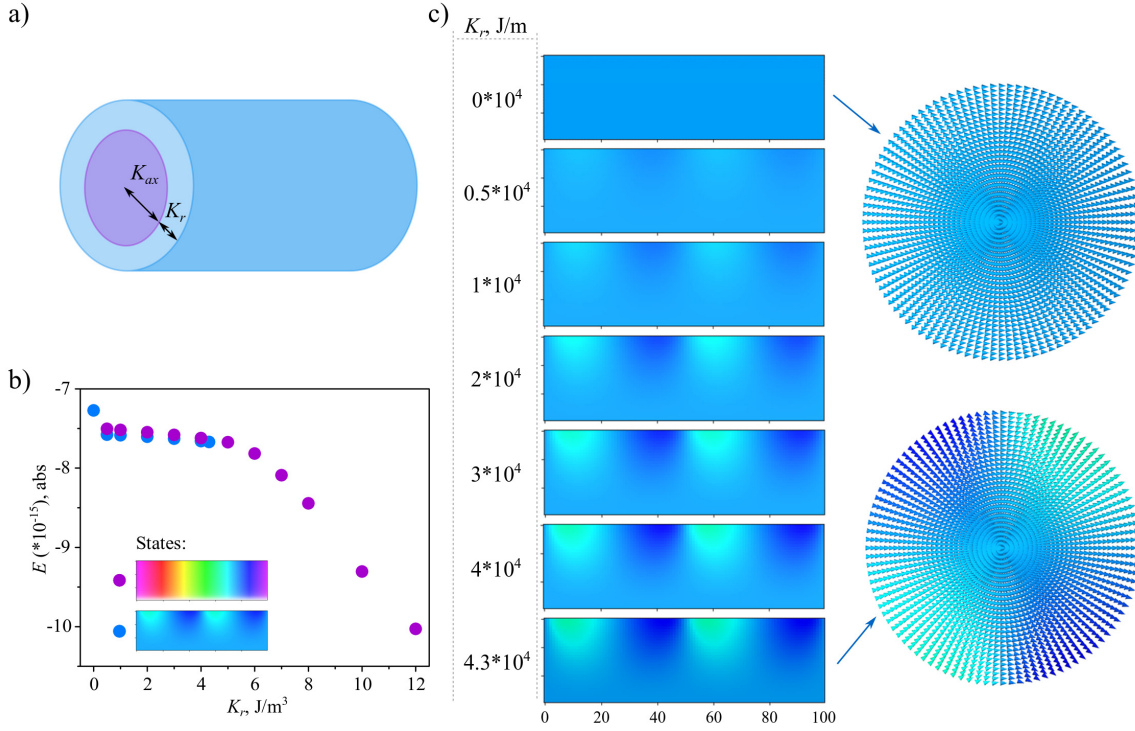


FIG. 3. a) Schematic representation of a cylindrical wire showing the distribution of various types of anisotropy, K_{ax} is axial anisotropy (purple part), K_r is radial anisotropy (blue part). Black arrows show the area (volume) of the wire occupied by each type of anisotropy; b) Dependence of wire energy on the magnitude of radial anisotropy for two configurations of DW. Radial DW exists in the entire range of considered anisotropy values except $K_r = 0$, while transverse DW only exists in the range from 0 to $4.3 \cdot 10^4$ J/m for the wire parameters considered in the work; c) Evolution of the magnetic configuration of the transverse DW with a change of the radial anisotropy value. For each radial anisotropy value, an unrolled view of the $\rho - \phi$ DW cross section is given.

from the original direction near the wire surface, which becomes more pronounced as the radial anisotropy increases. For the limiting case, when $K_r = 4.3 \cdot 10^4$ J/m, the angle of rotation of the magnetization at the periphery from the initial one (at $K_r = 0$ J/m) is almost $+90^\circ$ and -90° , while in the center the direction of magnetization remains original. A further increase in radial anisotropy leads to stabilization of the radial DW.

4. Conclusion

We found two different domain wall configurations in cylindrical wires with inhomogeneous anisotropy. One of them is a transverse domain wall, the other is a so-called radial domain wall, where the magnetization has a Bloch point in the wire center. Phase diagrams of stable configurations of domain walls for wires with different radial anisotropy in the near-surface region have been constructed. A change in the internal structure of the transverse domain wall was found in the presence of nonzero radial anisotropy in the near-surface region of the wire.

There is a certain range of parameter values in which both types of DW are locally stable and have close energy. Transitions between these states are possible due to thermal fluctuations and random perturbations. The rate of such transitions can be estimated based on transition state theory (TST) for magnetic degrees of freedom [25]. In harmonic approximation of TST the temperature dependence of transition rate is given by the Arrhenius law. Activation barrier for transition between different type of DW can be found after building the minimal energy path between correspondent locally stable states on the multidimensional energy surface of the system. The maximum along the path corresponds to the saddle point on the multidimensional energy surface. The difference between the energies in saddle point and initial state determines the activation energy for transition whereas the preexponential factor depend on the shape of the energy surface near these points [26].

References

- [1] Parkin S.S.P., Hayashi M. and Thomas L. Magnetic Domain-Wall Racetrack Memory. *Science*, 2008, **320**, 5873, P. 190–194.
- [2] Parkin S., Yang S.H. Memory on the racetrack. *Nature nanotechnology*, 2015, 10(3), P. 195–198.
- [3] Blasing R. et al. Magnetic Racetrack Memory: From Physics to the Cusp of Applications Within a Decade. *Proc. IEEE*, 2020, **108**, P. 1303–1321.
- [4] Alam J., et.al. Cylindrical micro and nanowires: Fabrication, properties and applications. *J. Magn. Magn. Mater.*, 2020, **513**, P. 167074.

- [5] Hertel R., Computational micromagnetism of magnetization processes in nickel nanowires. *J. Magn. Magn. Mater.*, 2002, **249**(1-2), P. 251–256.
- [6] Ferguson C.A., MacLaren D.A., McVitie S. Metastable magnetic domain walls in cylindrical nanowires. *J. Magn. Magn. Mater.*, 2015, **381**, P. 457–462.
- [7] Yan M. Beating the Walker limit with massless domain walls in cylindrical nanowires. *Phys. Rev. Lett.*, 2010, **104**, P. 057201.
- [8] Mougín A., Cormier M., Adam J. P., Metaxas P. J. and Ferre J. Domain wall mobility, stability and Walker breakdown in magnetic nanowires. *EPL*, 2007, **78**, P. 57007.
- [9] Hertel R. Ultrafast domain wall dynamics in magnetic nanotubes and nanowires. *J. Phys.: Condens. Matter*, 2016, **28**, P. 483002.
- [10] Yan M., Andreas C., Kakay A., Garcia-Sanchez F., Hertel R. Fast domain wall dynamics in magnetic nanotubes: Suppression of Walker breakdown and Cherenkov-like spin wave emission. *Appl. Phys. Lett.*, 2011, **99**, P. 122505.
- [11] Bukharaev A.A., Zvezdin A.K., Pyatakov A.P., Fetisov Y.K. Straintronics: a new trend in micro- and nanoelectronics and materials science. *Physics-Uspekhi*, 2018, **61**(12), P. 1175.
- [12] Larin V.S., Torcunov A.V., Zhukov A., Gonzalez J., Vazquez M., Panina L. Preparation and properties of glass-coated microwires. *J. Magn. Magn. Mater.*, 2002, **249**(1-2), P. 39-45.
- [13] Zhukov A., Gonzalez J., Blanco J.M., Vazquez M., Larin V. Microwires coated by glass: a new family of soft and hard magnetic materials. *J. Mater. Res.*, 2000, **15**, P. 2107-2113
- [14] Zhukova V., Ipatov M., Zhukov A. Thin magnetically soft wires for magnetic microsensors. *Sensors*, 2009, **9**, P. 9216-2940.
- [15] Baranov S.A., Larin V.S., Torcunov A.V. Technology, Preparation and Properties of the Cast Glass-Coated Magnetic Microwires. *Crystals*, 2017, **7**(6), P. 136.
- [16] Chiriac H., Ovari T.A., Pop Gh. Internal stress distribution in glass-covered amorphous magnetic wires. *Phys. Rev. B.*, 1995, **52**(14), P. 10104.
- [17] Chiriac H., Ovari T.A., Zhukov A. Magnetoelastic anisotropy of amorphous microwires. *J. Magn. Magn. Mater.*, 2003, **496**, P. 254-255.
- [18] Zhukova V., Blanco J.M., Ipatov M., Zhukov A. Magnetoelastic contribution in domain wall dynamics of amorphous microwires. *Physica B*, 2012, **407**, P. 1450–1454.
- [19] Corte-León P., Gonzalez-Legarreta L., Zhukova V., Ipatov M., Blanco J. M., Churyukanova M., Taskaev S. and Zhukov A. Controlling the domain wall dynamics in Fe-, Ni- and Co- based magnetic microwires. *J. Alloys Compound.*, 2020, **834**, P. 155170.
- [20] Zhukova, V., Corte-Leon, P., González-Legarreta, L., Talaat, A., Blanco, J.M., Ipatov, M., Olivera, J. and Zhukov, A. Review of domain wall dynamics engineering in magnetic microwires. *Nanomaterials*, 2020, **10**(12), P. 2407.
- [21] Corte-León, P., Zhukova V., Blanco J.M., Chizhik A., Ipatov M., Gonzalez J., Fert A., Alonso A. and Zhukov A. Engineering of domain wall propagation in magnetic microwires with graded magnetic anisotropy. *Applied Materials Today*, 2022, **26**, P. 101263.
- [22] Chichay K., et. al. Tunable domain wall dynamics in amorphous ferromagnetic microwires. *J. Alloys Compound.*, 2020, **835**, P. 154843.
- [23] Gudoshnikov S.A., Grebenshchikov Yu.B., Ljubimov B.Ya., Palvanov P.S., Usov N.A., Ipatov M., Zhukov A., Gonzalez J. Ground state magnetization distribution and characteristic width of head to head domain wall in Fe-rich amorphous microwire. *Phys. Stat. Sol. A*, 2009, **206**(4), P. 613-617.
- [24] Panina L.V., Ipatov M., Zhukova V., Zhukov A. Domain wall propagation in Fe-rich amorphous microwires. *Physica B*, 2012, **407**(4), P. 1442–1445.
- [25] Lobanov I.S., Potkina M.N., Uzdin V.M. Stability and Lifetimes of Magnetic States of Nano- and Microstructures (Brief Review). *JETP Letters*, 2021, **113**(12), P. 801–813.
- [26] Lobanov I.S., Uzdin V.M. The lifetime of micron scale topological chiral magnetic states with atomic resolution. *Comp. Phys. Commun.*, 2021, **269**, P. 108136.

Submitted 11 November 2023; revised 1 December 2023; accepted 7 December 2023

Information about the authors:

Ksenia A. Chichay – Department of Physics, ITMO University, St. Petersburg, 197101, Russia; ORCID 0000-0002-6921-6075; ks.chichay@gmail.com

Igor S. Lobanov – Department of Physics, ITMO University, St. Petersburg, 197101, Russia; ORCID 0000-0001-8789-3267; lobanov.igor@gmail.com

Valery M. Uzdin – Department of Physics, ITMO University, St. Petersburg, 197101, Russia; ORCID 0000-0002-9505-0996; v.uzdin@mail.ru

Conflict of interest: the authors declare no conflict of interest.